

Study of $B \rightarrow X\gamma$ Decays and Determination of $|V_{td}/V_{ts}|$

P. del Amo Sanchez,¹ J. P. Lees,¹ V. Poireau,¹ E. Prencipe,¹ V. Tisserand,¹ J. Garra Tico,² E. Grauges,² M. Martinelli^{ab,3}, A. Palano^{ab,3}, M. Pappagallo^{ab,3}, G. Eigen,⁴ B. Stugu,⁴ L. Sun,⁴ M. Battaglia,⁵ D. N. Brown,⁵ B. Hooberman,⁵ L. T. Kerth,⁵ Yu. G. Kolomensky,⁵ G. Lynch,⁵ I. L. Osipenkov,⁵ T. Tanabe,⁵ C. M. Hawkes,⁶ A. T. Watson,⁶ H. Koch,⁷ T. Schroeder,⁷ D. J. Asgeirsson,⁸ C. Hearty,⁸ T. S. Mattison,⁸ J. A. McKenna,⁸ A. Khan,⁹ A. Randle-Conde,⁹ V. E. Blinov,¹⁰ A. R. Buzykaev,¹⁰ V. P. Druzhinin,¹⁰ V. B. Golubev,¹⁰ A. P. Onuchin,¹⁰ S. I. Serednyakov,¹⁰ Yu. I. Skovpen,¹⁰ E. P. Solodov,¹⁰ K. Yu. Todyshev,¹⁰ A. N. Yushkov,¹⁰ M. Bondioli,¹¹ S. Curry,¹¹ D. Kirkby,¹¹ A. J. Lankford,¹¹ M. Mandelkern,¹¹ E. C. Martin,¹¹ D. P. Stoker,¹¹ H. Atmacan,¹² J. W. Gary,¹² F. Liu,¹² O. Long,¹² G. M. Vitug,¹² C. Campagnari,¹³ T. M. Hong,¹³ D. Kovalskiy,¹³ J. D. Richman,¹³ A. M. Eisner,¹⁴ C. A. Heusch,¹⁴ J. Kroseberg,¹⁴ W. S. Lockman,¹⁴ A. J. Martinez,¹⁴ T. Schalk,¹⁴ B. A. Schumm,¹⁴ A. Seiden,¹⁴ L. O. Winstrom,¹⁴ C. H. Cheng,¹⁵ D. A. Doll,¹⁵ B. Echenard,¹⁵ D. G. Hitlin,¹⁵ P. Ongmongkolkul,¹⁵ F. C. Porter,¹⁵ A. Y. Rakitin,¹⁵ R. Andreassen,¹⁶ M. S. Dubrovin,¹⁶ G. Mancinelli,¹⁶ B. T. Meadows,¹⁶ M. D. Sokoloff,¹⁶ P. C. Bloom,¹⁷ W. T. Ford,¹⁷ A. Gaz,¹⁷ J. F. Hirschauer,¹⁷ M. Nagel,¹⁷ U. Nauenberg,¹⁷ J. G. Smith,¹⁷ S. R. Wagner,¹⁷ R. Ayad,^{18,*} W. H. Toki,¹⁸ T. M. Karbach,¹⁹ J. Merkel,¹⁹ A. Petzold,¹⁹ B. Spaan,¹⁹ K. Wacker,¹⁹ M. J. Kobel,²⁰ K. R. Schubert,²⁰ R. Schwierz,²⁰ D. Bernard,²¹ M. Verderi,²¹ P. J. Clark,²² S. Playfer,²² J. E. Watson,²² M. Andreotti^{ab,23}, D. Bettoni^{a,23}, C. Bozzi^{a,23}, R. Calabrese^{ab,23}, A. Cecchi^{ab,23}, G. Cibinetto^{ab,23}, E. Fioravanti^{ab,23}, P. Franchini^{ab,23}, E. Luppi^{ab,23}, M. Murerato^{ab,23}, M. Negrini^{ab,23}, A. Petrella^{ab,23}, L. Piemontese^{a,23}, R. Baldini-Ferrolli,²⁴ A. Calcaterra,²⁴ R. de Sangro,²⁴ G. Finocchiaro,²⁴ M. Nicolaci,²⁴ S. Pacetti,²⁴ P. Patteri,²⁴ I. M. Peruzzi,^{24,†} M. Piccolo,²⁴ M. Rama,²⁴ A. Zallo,²⁴ R. Contri^{ab,25}, E. Guido^{ab,25}, M. Lo Vetere^{ab,25}, M. R. Monge^{ab,25}, S. Passaggio^{a,25}, C. Patrignani^{ab,25}, E. Robutti^{a,25}, S. Tosi^{ab,25}, B. Bhuyan,²⁶ C. L. Lee,²⁷ M. Morii,²⁷ A. Adametz,²⁸ J. Marks,²⁸ S. Schenk,²⁸ U. Uwer,²⁸ F. U. Bernlochner,²⁹ M. Ebert,²⁹ H. M. Lacker,²⁹ T. Lueck,²⁹ A. Volk,²⁹ P. D. Dauncey,³⁰ M. Tibbetts,³⁰ P. K. Behera,³¹ U. Mallik,³¹ C. Chen,³² J. Cochran,³² H. B. Crawley,³² L. Dong,³² W. T. Meyer,³² S. Prell,³² E. I. Rosenberg,³² A. E. Rubin,³² Y. Y. Gao,³³ A. V. Gritsan,³³ Z. J. Guo,³³ N. Arnaud,³⁴ M. Davier,³⁴ D. Derkach,³⁴ J. Firmino da Costa,³⁴ G. Grosdidier,³⁴ F. Le Diberder,³⁴ A. M. Lutz,³⁴ B. Malaescu,³⁴ A. Perez,³⁴ P. Roudeau,³⁴ M. H. Schune,³⁴ J. Serrano,³⁴ V. Sordini,^{34,‡} A. Stocchi,³⁴ L. Wang,³⁴ G. Wormser,³⁴ D. J. Lange,³⁵ D. M. Wright,³⁵ I. Bingham,³⁶ J. P. Burke,³⁶ C. A. Chavez,³⁶ J. P. Coleman,³⁶ J. R. Fry,³⁶ E. Gabathuler,³⁶ R. Gamet,³⁶ D. E. Hutchcroft,³⁶ D. J. Payne,³⁶ C. Touramanis,³⁶ A. J. Bevan,³⁷ F. Di Lodovico,³⁷ R. Sacco,³⁷ M. Sigamani,³⁷ G. Cowan,³⁸ S. Paramesvaran,³⁸ A. C. Wren,³⁸ D. N. Brown,³⁹ C. L. Davis,³⁹ A. G. Denig,⁴⁰ M. Fritsch,⁴⁰ W. Gradl,⁴⁰ A. Hafner,⁴⁰ K. E. Alwyn,⁴¹ D. Bailey,⁴¹ R. J. Barlow,⁴¹ G. Jackson,⁴¹ G. D. Lafferty,⁴¹ T. J. West,⁴¹ J. Anderson,⁴² R. Cenci,⁴² A. Jawahery,⁴² D. A. Roberts,⁴² G. Simi,⁴² J. M. Tuggle,⁴² C. Dallapiccola,⁴³ E. Salvati,⁴³ R. Cowan,⁴⁴ D. Dujmic,⁴⁴ P. H. Fisher,⁴⁴ G. Sciolla,⁴⁴ M. Zhao,⁴⁴ D. Lindemann,⁴⁵ P. M. Patel,⁴⁵ S. H. Robertson,⁴⁵ M. Schram,⁴⁵ P. Biassoni^{ab,46}, A. Lazzaro^{ab,46}, V. Lombardo^{ab,46}, F. Palombo^{ab,46}, S. Stracka^{ab,46}, L. Cremaldi,⁴⁷ R. Godang,^{47,§} R. Kroeger,⁴⁷ P. Sonnek,⁴⁷ D. J. Summers,⁴⁷ X. Nguyen,⁴⁸ M. Simard,⁴⁸ P. Taras,⁴⁸ G. De Nardo^{ab,49}, D. Monorchio^{ab,49}, G. Onorato^{ab,49}, C. Sciacca^{ab,49}, G. Raven,⁵⁰ H. L. Snoek,⁵⁰ C. P. Jessop,⁵¹ K. J. Knoepfel,⁵¹ J. M. LoSecco,⁵¹ W. F. Wang,⁵¹ L. A. Corwin,⁵² K. Honscheid,⁵² R. Kass,⁵² J. P. Morris,⁵² A. M. Rahimi,⁵² N. L. Blount,⁵³ J. Brau,⁵³ R. Frey,⁵³ O. Igonkina,⁵³ J. A. Kolb,⁵³ R. Rahmat,⁵³ N. B. Sinev,⁵³ D. Strom,⁵³ J. Strube,⁵³ E. Torrence,⁵³ G. Castelli^{ab,54}, E. Feltresi^{ab,54}, N. Gagliardi^{ab,54}, M. Margoni^{ab,54}, M. Morandin^{a,54}, M. Posocco^{a,54}, M. Rotondo^{a,54}, F. Simonetto^{ab,54}, R. Stroili^{ab,54}, E. Ben-Haim,⁵⁵ G. R. Bonneaud,⁵⁵ H. Briand,⁵⁵ G. Calderini,⁵⁵ J. Chauveau,⁵⁵ O. Hamon,⁵⁵ Ph. Leruste,⁵⁵ G. Marchiori,⁵⁵ J. Ocariz,⁵⁵ J. Prendki,⁵⁵ S. Sitt,⁵⁵ M. Biasini^{ab,56}, E. Manoni^{ab,56}, C. Angelini^{ab,57}, G. Batignani^{ab,57}, S. Bettarini^{ab,57}, M. Carpinelli^{ab,57}, ¶ G. Casarosa^{ab,57}, A. Cervelli^{ab,57}, F. Forti^{ab,57}, M. A. Giorgi^{ab,57}, A. Lusiani^{ac,57}, N. Neri^{ab,57}, E. Paoloni^{ab,57}, G. Rizzo^{ab,57}, J. J. Walsh^{a,57}, D. Lopes Pegna,⁵⁸ C. Lu,⁵⁸ J. Olsen,⁵⁸ A. J. S. Smith,⁵⁸ A. V. Telnov,⁵⁸ F. Anulli^{a,59}, E. Baracchini^{ab,59}, G. Cavoto^{a,59}, R. Faccini^{ab,59}, F. Ferrarotto^{a,59}, F. Ferroni^{ab,59}, M. Gaspero^{ab,59}, L. Li Gioi^{a,59}, M. A. Mazzoni^{a,59}, G. Piredda^{a,59}, F. Renga^{ab,59}, T. Hartmann,⁶⁰ T. Leddig,⁶⁰ H. Schröder,⁶⁰ R. Waldi,⁶⁰ T. Adye,⁶¹ B. Franek,⁶¹ E. O. Olaiya,⁶¹ F. F. Wilson,⁶¹ S. Emery,⁶² G. Hamel de Monchenault,⁶² G. Vasseur,⁶² Ch. Yèche,⁶² M. Zito,⁶² M. T. Allen,⁶³ D. Aston,⁶³ D. J. Bard,⁶³ R. Bartoldus,⁶³ J. F. Benitez,⁶³ C. Cartaro,⁶³ M. R. Convery,⁶³ J. Dorfan,⁶³ G. P. Dubois-Felsmann,⁶³ W. Dunwoodie,⁶³ R. C. Field,⁶³ M. Franco Sevilla,⁶³ B. G. Fulsom,⁶³ A. M. Gabareen,⁶³ M. T. Graham,⁶³ P. Grenier,⁶³ C. Hast,⁶³ W. R. Innes,⁶³ M. H. Kelsey,⁶³ H. Kim,⁶³

P. Kim,⁶³ M. L. Kocian,⁶³ D. W. G. S. Leith,⁶³ S. Li,⁶³ B. Lindquist,⁶³ S. Luitz,⁶³ V. Luth,⁶³ H. L. Lynch,⁶³ D. B. MacFarlane,⁶³ H. Marsiske,⁶³ D. R. Muller,⁶³ H. Neal,⁶³ S. Nelson,⁶³ C. P. O'Grady,⁶³ I. Ofte,⁶³ M. Perl,⁶³ T. Pulliam,⁶³ B. N. Ratcliff,⁶³ A. Roodman,⁶³ A. A. Salnikov,⁶³ V. Santoro,⁶³ R. H. Schindler,⁶³ J. Schwiening,⁶³ A. Snyder,⁶³ D. Su,⁶³ M. K. Sullivan,⁶³ S. Sun,⁶³ K. Suzuki,⁶³ J. M. Thompson,⁶³ J. Va'vra,⁶³ A. P. Wagner,⁶³ M. Weaver,⁶³ C. A. West,⁶³ W. J. Wisniewski,⁶³ M. Wittgen,⁶³ D. H. Wright,⁶³ H. W. Wulsin,⁶³ A. K. Yarritu,⁶³ C. C. Young,⁶³ V. Ziegler,⁶³ X. R. Chen,⁶⁴ W. Park,⁶⁴ M. V. Purohit,⁶⁴ R. M. White,⁶⁴ J. R. Wilson,⁶⁴ S. J. Sekula,⁶⁵ M. Bellis,⁶⁶ P. R. Burchat,⁶⁶ A. J. Edwards,⁶⁶ T. S. Miyashita,⁶⁶ S. Ahmed,⁶⁷ M. S. Alam,⁶⁷ J. A. Ernst,⁶⁷ B. Pan,⁶⁷ M. A. Saeed,⁶⁷ S. B. Zain,⁶⁷ N. Guttman,⁶⁸ A. Soffer,⁶⁸ P. Lund,⁶⁹ S. M. Spanier,⁶⁹ R. Eckmann,⁷⁰ J. L. Ritchie,⁷⁰ A. M. Ruland,⁷⁰ C. J. Schilling,⁷⁰ R. F. Schwitters,⁷⁰ B. C. Wray,⁷⁰ J. M. Izen,⁷¹ X. C. Lou,⁷¹ F. Bianchi^{ab,72} D. Gamba^{ab,72} M. Pelliccioni^{ab,72} M. Bomben^{ab,73} L. Lanceri^{ab,73} L. Vitale^{ab,73} N. Lopez-March,⁷⁴ F. Martinez-Vidal,⁷⁴ D. A. Milanes,⁷⁴ A. Oyanguren,⁷⁴ J. Albert,⁷⁵ Sw. Banerjee,⁷⁵ H. H. F. Choi,⁷⁵ K. Hamano,⁷⁵ G. J. King,⁷⁵ R. Kowalewski,⁷⁵ M. J. Lewczuk,⁷⁵ I. M. Nugent,⁷⁵ J. M. Roney,⁷⁵ R. J. Sobie,⁷⁵ T. J. Gershon,⁷⁶ P. F. Harrison,⁷⁶ J. Ilic,⁷⁶ T. E. Latham,⁷⁶ E. M. T. Puccio,⁷⁶ H. R. Band,⁷⁷ X. Chen,⁷⁷ S. Dasu,⁷⁷ K. T. Flood,⁷⁷ Y. Pan,⁷⁷ R. Prepost,⁷⁷ C. O. Vuosalo,⁷⁷ and S. L. Wu⁷⁷

(The BABAR Collaboration)

¹Laboratoire d'Annecy-le-Vieux de Physique des Particules (LAPP),
Université de Savoie, CNRS/IN2P3, F-74941 Annecy-Le-Vieux, France

²Universitat de Barcelona, Facultat de Física, Departament ECM, E-08028 Barcelona, Spain

³INFN Sezione di Bari^a; Dipartimento di Fisica, Università di Bari^b, I-70126 Bari, Italy

⁴University of Bergen, Institute of Physics, N-5007 Bergen, Norway

⁵Lawrence Berkeley National Laboratory and University of California, Berkeley, California 94720, USA

⁶University of Birmingham, Birmingham, B15 2TT, United Kingdom

⁷Ruhr Universität Bochum, Institut für Experimentalphysik 1, D-44780 Bochum, Germany

⁸University of British Columbia, Vancouver, British Columbia, Canada V6T 1Z1

⁹Brunel University, Uxbridge, Middlesex UB8 3PH, United Kingdom

¹⁰Budker Institute of Nuclear Physics, Novosibirsk 630090, Russia

¹¹University of California at Irvine, Irvine, California 92697, USA

¹²University of California at Riverside, Riverside, California 92521, USA

¹³University of California at Santa Barbara, Santa Barbara, California 93106, USA

¹⁴University of California at Santa Cruz, Institute for Particle Physics, Santa Cruz, California 95064, USA

¹⁵California Institute of Technology, Pasadena, California 91125, USA

¹⁶University of Cincinnati, Cincinnati, Ohio 45221, USA

¹⁷University of Colorado, Boulder, Colorado 80309, USA

¹⁸Colorado State University, Fort Collins, Colorado 80523, USA

¹⁹Technische Universität Dortmund, Fakultät Physik, D-44221 Dortmund, Germany

²⁰Technische Universität Dresden, Institut für Kern- und Teilchenphysik, D-01062 Dresden, Germany

²¹Laboratoire Leprince-Ringuet, CNRS/IN2P3, Ecole Polytechnique, F-91128 Palaiseau, France

²²University of Edinburgh, Edinburgh EH9 3JZ, United Kingdom

²³INFN Sezione di Ferrara^a; Dipartimento di Fisica, Università di Ferrara^b, I-44100 Ferrara, Italy

²⁴INFN Laboratori Nazionali di Frascati, I-00044 Frascati, Italy

²⁵INFN Sezione di Genova^a; Dipartimento di Fisica, Università di Genova^b, I-16146 Genova, Italy

²⁶Indian Institute of Technology Guwahati, Guwahati, Assam, 781 039, India

²⁷Harvard University, Cambridge, Massachusetts 02138, USA

²⁸Universität Heidelberg, Physikalisches Institut, Philosophenweg 12, D-69120 Heidelberg, Germany

²⁹Humboldt-Universität zu Berlin, Institut für Physik, Newtonstr. 15, D-12489 Berlin, Germany

³⁰Imperial College London, London, SW7 2AZ, United Kingdom

³¹University of Iowa, Iowa City, Iowa 52242, USA

³²Iowa State University, Ames, Iowa 50011-3160, USA

³³Johns Hopkins University, Baltimore, Maryland 21218, USA

³⁴Laboratoire de l'Accélérateur Linéaire, IN2P3/CNRS et Université Paris-Sud 11,

Centre Scientifique d'Orsay, B. P. 34, F-91898 Orsay Cedex, France

³⁵Lawrence Livermore National Laboratory, Livermore, California 94550, USA

³⁶University of Liverpool, Liverpool L69 7ZE, United Kingdom

³⁷Queen Mary, University of London, London, E1 4NS, United Kingdom

³⁸University of London, Royal Holloway and Bedford New College, Egham, Surrey TW20 0EX, United Kingdom

³⁹University of Louisville, Louisville, Kentucky 40292, USA

⁴⁰Johannes Gutenberg-Universität Mainz, Institut für Kernphysik, D-55099 Mainz, Germany

⁴¹University of Manchester, Manchester M13 9PL, United Kingdom

⁴²University of Maryland, College Park, Maryland 20742, USA

⁴³University of Massachusetts, Amherst, Massachusetts 01003, USA

- ⁴⁴Massachusetts Institute of Technology, Laboratory for Nuclear Science, Cambridge, Massachusetts 02139, USA
⁴⁵McGill University, Montréal, Québec, Canada H3A 2T8
⁴⁶INFN Sezione di Milano^a; Dipartimento di Fisica, Università di Milano^b, I-20133 Milano, Italy
⁴⁷University of Mississippi, University, Mississippi 38677, USA
⁴⁸Université de Montréal, Physique des Particules, Montréal, Québec, Canada H3C 3J7
⁴⁹INFN Sezione di Napoli^a; Dipartimento di Scienze Fisiche, Università di Napoli Federico II^b, I-80126 Napoli, Italy
⁵⁰NIKHEF, National Institute for Nuclear Physics and High Energy Physics, NL-1009 DB Amsterdam, The Netherlands
⁵¹University of Notre Dame, Notre Dame, Indiana 46556, USA
⁵²Ohio State University, Columbus, Ohio 43210, USA
⁵³University of Oregon, Eugene, Oregon 97403, USA
⁵⁴INFN Sezione di Padova^a; Dipartimento di Fisica, Università di Padova^b, I-35131 Padova, Italy
⁵⁵Laboratoire de Physique Nucléaire et de Hautes Energies, IN2P3/CNRS, Université Pierre et Marie Curie-Paris6, Université Denis Diderot-Paris7, F-75252 Paris, France
⁵⁶INFN Sezione di Perugia^a; Dipartimento di Fisica, Università di Perugia^b, I-06100 Perugia, Italy
⁵⁷INFN Sezione di Pisa^a; Dipartimento di Fisica, Università di Pisa^b; Scuola Normale Superiore di Pisa^c, I-56127 Pisa, Italy
⁵⁸Princeton University, Princeton, New Jersey 08544, USA
⁵⁹INFN Sezione di Roma^a; Dipartimento di Fisica, Università di Roma La Sapienza^b, I-00185 Roma, Italy
⁶⁰Universität Rostock, D-18051 Rostock, Germany
⁶¹Rutherford Appleton Laboratory, Chilton, Didcot, Oxon, OX11 0QX, United Kingdom
⁶²CEA, Irfu, SPP, Centre de Saclay, F-91191 Gif-sur-Yvette, France
⁶³SLAC National Accelerator Laboratory, Stanford, California 94309 USA
⁶⁴University of South Carolina, Columbia, South Carolina 29208, USA
⁶⁵Southern Methodist University, Dallas, Texas 75275, USA
⁶⁶Stanford University, Stanford, California 94305-4060, USA
⁶⁷State University of New York, Albany, New York 12222, USA
⁶⁸Tel Aviv University, School of Physics and Astronomy, Tel Aviv, 69978, Israel
⁶⁹University of Tennessee, Knoxville, Tennessee 37996, USA
⁷⁰University of Texas at Austin, Austin, Texas 78712, USA
⁷¹University of Texas at Dallas, Richardson, Texas 75083, USA
⁷²INFN Sezione di Torino^a; Dipartimento di Fisica Sperimentale, Università di Torino^b, I-10125 Torino, Italy
⁷³INFN Sezione di Trieste^a; Dipartimento di Fisica, Università di Trieste^b, I-34127 Trieste, Italy
⁷⁴IFIC, Universitat de Valencia-CSIC, E-46071 Valencia, Spain
⁷⁵University of Victoria, Victoria, British Columbia, Canada V8W 3P6
⁷⁶Department of Physics, University of Warwick, Coventry CV4 7AL, United Kingdom
⁷⁷University of Wisconsin, Madison, Wisconsin 53706, USA

Using a sample of 471 million $B\bar{B}$ events collected with the BABAR detector, we study the sum of seven exclusive final states $B \rightarrow X_{s(d)}\gamma$, where $X_{s(d)}$ is a strange (non-strange) hadronic system with a mass of up to 2.0 GeV/ c^2 . After correcting for unobserved decay modes, we obtain a branching fraction for $b \rightarrow d\gamma$ of $(9.2 \pm 2.0(stat.) \pm 2.3(syst.)) \times 10^{-6}$ in this mass range, and a branching fraction for $b \rightarrow s\gamma$ of $(23.0 \pm 0.8(stat.) \pm 3.0(syst.)) \times 10^{-5}$ in the same mass range. We find $\frac{\mathcal{B}(b \rightarrow d\gamma)}{\mathcal{B}(b \rightarrow s\gamma)} = 0.040 \pm 0.009(stat.) \pm 0.010(syst.)$, from which we determine $|V_{td}/V_{ts}| = 0.199 \pm 0.022(stat.) \pm 0.024(syst.) \pm 0.002(th.)$.

PACS numbers:

The decays $b \rightarrow d\gamma$ and $b \rightarrow s\gamma$ are flavor-changing neutral current processes forbidden at tree level in the

Standard Model (SM). The leading-order processes are one-loop electroweak penguin diagrams, for which the top quark is the dominant virtual particle. In theories beyond the SM, new virtual particles may appear in the loop, which could lead to measurable effects on experimental observables such as branching fractions and CP asymmetries [1]. In the SM the inclusive rate for $b \rightarrow d\gamma$ is suppressed relative to $b \rightarrow s\gamma$ by a factor $|V_{td}/V_{ts}|^2$, where V_{td} and V_{ts} are Cabibbo-Kobayashi-Maskawa matrix elements. Measurements of $|V_{td}/V_{ts}|$ using the exclusive modes $B \rightarrow (\rho, \omega)\gamma$ and $B \rightarrow K^*\gamma$ [4, 5] are now well-established, with theoretical uncertainties of 7% from

*Now at Temple University, Philadelphia, Pennsylvania 19122, USA

†Also with Università di Perugia, Dipartimento di Fisica, Perugia, Italy

‡Also with Università di Roma La Sapienza, I-00185 Roma, Italy

§Now at University of South Alabama, Mobile, Alabama 36688, USA

¶Also with Università di Sassari, Sassari, Italy

TABLE I: The reconstructed decay modes. Charge conjugate states are implied throughout this paper.

| | |
|--|--|
| $B \rightarrow X_d \gamma$ | $B \rightarrow X_s \gamma$ |
| $B^0 \rightarrow \pi^+ \pi^- \gamma$ | $B^0 \rightarrow K^+ \pi^- \gamma$ |
| $B^+ \rightarrow \pi^+ \pi^0 \gamma$ | $B^+ \rightarrow K^+ \pi^0 \gamma$ |
| $B^+ \rightarrow \pi^+ \pi^- \pi^+ \gamma$ | $B^+ \rightarrow K^+ \pi^+ \pi^- \gamma$ |
| $B^0 \rightarrow \pi^+ \pi^- \pi^0 \gamma$ | $B^0 \rightarrow K^+ \pi^- \pi^0 \gamma$ |
| $B^0 \rightarrow \pi^+ \pi^- \pi^+ \pi^- \gamma$ | $B^0 \rightarrow K^+ \pi^- \pi^+ \pi^- \gamma$ |
| $B^+ \rightarrow \pi^+ \pi^- \pi^+ \pi^0 \gamma$ | $B^+ \rightarrow K^+ \pi^- \pi^+ \pi^0 \gamma$ |
| $B^+ \rightarrow \pi^+ \eta \gamma$ | $B^+ \rightarrow K^+ \eta \gamma$ |

weak annihilation and hadronic form factors [2]. This ratio can also be obtained from the B_d and B_s mixing frequencies [3]. It is important to confirm the consistency of the two methods of determining $|V_{td}/V_{ts}|$, since new physics effects would enter in different ways in mixing and radiative decays. A measurement of the branching fractions of inclusive $b \rightarrow d\gamma$ relative to $b \rightarrow s\gamma$ would determine $|V_{td}/V_{ts}|$ with reduced theoretical uncertainties compared to that from exclusive modes [6].

This letter supersedes [8], and presents the first significant observation of the $b \rightarrow d\gamma$ transition in the hadronic mass range $M(X_d) > 1.0 \text{ GeV}/c^2$, resulting in a significant improvement in the determination of $|V_{td}/V_{ts}|$ via the ratio of inclusive widths. Inclusive $b \rightarrow s\gamma$ and $b \rightarrow d\gamma$ rates are extrapolated from the measurements of the partial decay rates to seven exclusive final states (see Table I) in the hadronic mass ranges $0.5 < M(X_d) < 1.0 \text{ GeV}/c^2$ (low mass, containing the previously measured K^* , ρ and ω resonances) and $1.0 < M(X_d) < 2.0 \text{ GeV}/c^2$ (high mass). We combine these measurements and make a model-dependent extrapolation to higher hadronic mass to obtain an inclusive branching fraction (\mathcal{B}) for $b \rightarrow (s, d)\gamma$. These measurements use the full dataset of 471×10^6 $B\bar{B}$ pairs collected at the $\Upsilon(4S)$ resonance at the PEP-II B factory with the BABAR detector [7].

High energy photons are reconstructed from an isolated energy cluster in the barrel of the calorimeter, with shape consistent with a single photon, and energy $1.15 < E_\gamma^* < 3.50 \text{ GeV}$, where $*$ denotes the center-of-mass (CM) frame. We remove photons that can form a π^0 (η) candidate in association with another photon of energy greater than 30 (250) MeV if the two-photon invariant mass is in the range $110 < m_{\gamma\gamma} < 160$ ($520 < m_{\gamma\gamma} < 560$) MeV/c^2 for the low mass region and $95 < m_{\gamma\gamma} < 155$ ($530 < m_{\gamma\gamma} < 565$) MeV/c^2 for the high mass region.

Charged pion and kaon candidates are selected from well-reconstructed tracks. We use a pion selection algorithm to differentiate pions from kaons, with a typical selection efficiency of 95% and kaon mis-identification rate of 4%. Kaons are identified as tracks failing the pion selection criteria. We reconstruct π^0 (η) candidates from pairs of photons of minimum energy 20 MeV with an invariant mass $115 < m_{\gamma\gamma} < 150$ ($470 < m_{\gamma\gamma} < 620$) MeV/c^2 . We require all pion, η and kaon candidates

to have a momentum in the laboratory frame greater than 600 (425) MeV/c in the low (high) mass region.

The selected pion, η , kaon and high-energy photon candidates are combined to form B meson candidates consistent with one of the seven decay modes. The charged particles are combined to form a common vertex with a χ^2 probability greater than 1%. We use the kinematic variables $\Delta E = E_B^* - E_{\text{beam}}^*$, where E_B^* is the energy of the B meson candidate and E_{beam}^* is the beam energy, and $m_{\text{ES}} = \sqrt{E_{\text{beam}}^{*2} - \vec{p}_B^{*2}}$, where \vec{p}_B^* is the momentum of the B candidate. We consider candidates in the range $-0.3 < \Delta E < 0.2 \text{ GeV}$ and $m_{\text{ES}} > 5.22 \text{ GeV}/c^2$.

Contributions from continuum processes ($e^+e^- \rightarrow q\bar{q}$, with $q = u, d, s, c$) are reduced by considering only events for which the ratio R_2 of second-to-zeroth order Fox-Wolfram moments [9] is less than 0.98. To further discriminate between the jet-like continuum background and the more spherically symmetric signal events, we compute the angle θ_T^* between the photon momentum and the thrust axis of the rest of the event (ROE) and require $|\cos(\theta_T^*)| < 0.8$. The ROE is defined as all charged tracks and neutral energy deposits that are not used to reconstruct the B candidate.

Ten other event shape variables that distinguish between signal and continuum events are combined in a neural network (NN). These include the ratio R_2' , which is R_2 is calculated in the frame recoiling against the photon momentum, the B meson production angle with respect to the beam axis in the CM frame, θ_B^* , and the L-moments [10] of the ROE with respect to either the thrust axis of the ROE or the direction of the high energy photon. Differences in lepton, pion and kaon production between background and B decays are exploited by including several flavor-tagging variables applied to the ROE [11]. Using the NN output, we reject 99% of continuum background while preserving 25% of signal decays

After all selections are applied, there remain events with more than one B candidate. In these events the candidate with the reconstructed π^0 or η mass closest to nominal is retained. Where there is no π^0 or η we retain the candidate with the highest vertex χ^2 probability.

The signal yields in the data for the sum of the seven decay modes are determined from two-dimensional extended maximum likelihood fits to the ΔE and m_{ES} distributions. We consider the following contributions: signal, combinatorial backgrounds from continuum processes, backgrounds from other B decays, and cross-feed from mis-reconstructed $B \rightarrow X\gamma$ decays. The fits to $B \rightarrow X_d\gamma$ events contain components from misidentified $b \rightarrow s\gamma$ decays, and we neglect the small $b \rightarrow d\gamma$ background in the fits to $B \rightarrow X_s\gamma$ events.

Each contribution is modeled by a probability density function (PDF) that is determined from Monte Carlo (MC) simulated events unless otherwise specified. For the misidentified signal cross-feed components, we use a binned two-dimensional PDF to account for correlations. All the other PDFs are products of one-dimensional func-

tions of ΔE and m_{ES} . For signal, the m_{ES} spectrum is described by a Crystal Ball function [12], and ΔE by a Cruiff function [13]. The parameters of these functions are determined from the fit to the high-statistics $B \rightarrow X_s \gamma$ data sample. We use these fitted values to fix the signal shape in the fits to $B \rightarrow X_d \gamma$ events.

The remaining B backgrounds contain a small component that peaks in m_{ES} but not ΔE , which is modeled by a Gaussian distribution in m_{ES} . Continuum and other non-peaking backgrounds are described by an ARGUS shape [14] in m_{ES} and a second-order polynomial in ΔE .

We perform separate fits for $B \rightarrow X_d \gamma$ and $B \rightarrow X_s \gamma$ in each of the hadronic mass ranges $0.5\text{-}1.0 \text{ GeV}/c^2$ and $1.0\text{-}2.0 \text{ GeV}/c^2$. For each of the four fits, we combine the component PDFs and fit for the signal, generic B and continuum yields, the ARGUS and two polynomial shape parameters. We scale the cross-feed contributions proportionally to the fitted signal yield, re-fit and iterate until the procedure converges. Projections of m_{ES} and ΔE from fits to data for $B \rightarrow X_s \gamma$ and $B \rightarrow X_d \gamma$ are shown in the high mass regions in Figure 1. Table II gives the signal yields, efficiencies (after corrections for systematic effects) and partial branching fractions (\mathcal{PB}). We calculate \mathcal{PB} using $\mathcal{PB}(B \rightarrow X\gamma) = N_S/(2 \epsilon N_{B\bar{B}})$, where $N_{B\bar{B}}$ is the number of $B\bar{B}$ pairs in the data sample.

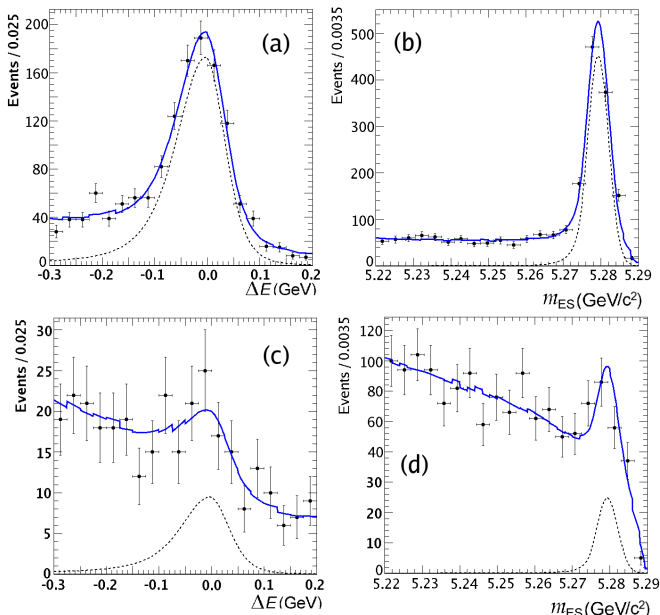


FIG. 1: Projections of ΔE with $5.275 < m_{ES} < 5.286 \text{ GeV}/c^2$ for (a) $B \rightarrow X_s \gamma$ and (b) $B \rightarrow X_d \gamma$, and of m_{ES} with $-0.1 < \Delta E < 0.05 \text{ GeV}$ for (c) $B \rightarrow X_s \gamma$ and (d) $B \rightarrow X_d \gamma$ in the mass range $1.0\text{-}2.0 \text{ GeV}/c^2$. Data points are compared with the sum of all the fit contributions (solid line). The jagged line is an artifact of the fit projection over the sum of several binned histograms. The dashed line shows the signal component.

We have investigated a number of sources of systematic uncertainty in the measurement of the partial branching

fractions, some of which are common to both $B \rightarrow X_d \gamma$ and $B \rightarrow X_s \gamma$ and cancel in the ratio of branching fractions (see Table III: those that do not cancel in the ratio are marked by an asterisk). Uncertainties in tracking efficiency, particle identification, γ and π^0 reconstruction, and the π^0/η veto have been evaluated using independent control samples of data and MC simulated events, and incorporated into our analysis. Uncertainty due to the NN selection has been evaluated by comparing the efficiency of the selection in data and MC for the $B \rightarrow X_s \gamma$ events, which are relatively free of background, assuming that potential discrepancies between data and MC are the same for the $B \rightarrow X_d \gamma$ sample. The means and widths of the signal PDF are varied within the range allowed by the fit to the $B \rightarrow X_s \gamma$ data, accounting for correlations. Other PDF parameters are also varied within the 1σ limits determined from the fit to MC. We vary the $b \rightarrow s\gamma$ background in the fit to $B \rightarrow X_d \gamma$ by the statistical uncertainty on our measurement of those decays. The signal cross-feed originating from our measured channels is varied by the statistical uncertainty on our measurement; other signal cross-feed backgrounds by $\pm 50\%$. An additional uncertainty on the efficiency arises from the fragmentation of the hadronic system among the measured final states. For $B \rightarrow X_s \gamma$ the uncertainty is constrained by the errors on the measured data; for $B \rightarrow X_d \gamma$ an estimate is obtained from the difference between the default phase-space fragmentation (see below) and a re-weighting using the measured data/MC differences in $B \rightarrow X_s \gamma$.

To obtain inclusive $\mathcal{B}(b \rightarrow s\gamma)$ and $\mathcal{B}(b \rightarrow d\gamma)$ we need to correct the partial \mathcal{B} values in Table II for the fractions of missing final states. After correcting for the 50% of missing decay modes with neutral kaons, the low mass $B \rightarrow X_s \gamma$ measurement is found to be consistent with previous measurements of the rate for $B \rightarrow K^* \gamma$ [15]. For the low mass $B \rightarrow X_d \gamma$ region, we correct for the small amount of non-reconstructed ω final states (for example, $\omega \rightarrow \pi^0 \gamma$), and find a partial branching fraction consistent with previous measurements of $\mathcal{B}(B \rightarrow (\rho, \omega) \gamma)$ [15]. We assume that non-resonant decays do not contribute in this region.

In the high mass region, the missing fractions depend on the fragmentation of the hadronic system and are expected to be different for X_d and X_s . In our signal MC, fragmentation is modeled by selecting an array of final-state particles and resonances according to the phase-space probability of the final state, as implemented by JETSET [16]. We further constrain the distribution of X_s final states to that observed for our seven decay modes as well as the distributions of a number of other states measured in [17]. According to this MC model we reconstruct 43% of the total width in $b \rightarrow d\gamma$, and 36% in $b \rightarrow s\gamma$. A further 37% of the width of $b \rightarrow s\gamma$ is constrained by the isospin relation between charged and neutral kaon decays. We explore the uncertainty in the correction for missing modes by considering several alternative models: replacing 50% of $b \rightarrow s\gamma$ and $b \rightarrow d\gamma$

TABLE II: Signal yields (N_S), efficiencies (ϵ), partial branching fractions ($\mathcal{P}\mathcal{B}$), inclusive branching fractions (\mathcal{B}) and the ratio of inclusive branching fractions for the measured decay modes. The first error is statistical and second is systematic (including an error from extrapolation to missing decay modes, for the inclusive \mathcal{B}).

| | $M(X_s)0.5-1.0$ | $M(X_d)0.5-1.0$ | $M(X_s)1.0-2.0$ | $M(X_d)1.0-2.0$ | $M(X_s)0.5-2.0$ | $M(X_d)0.5-2.0$ |
|---|-----------------------------|-----------------------|--------------------|-----------------------|-----------------------------|-----------------------|
| N_S | 804 ± 33 | 35 ± 9 | 990 ± 42 | 56 ± 14 | - | - |
| ϵ | 4.5% | 3.1% | 1.6% | 1.9% | - | - |
| $\mathcal{P}\mathcal{B}(\times 10^{-6})$ | $19 \pm 1 \pm 1$ | $1.2 \pm 0.3 \pm 0.1$ | $66 \pm 3 \pm 6$ | $3.2 \pm 0.8 \pm 0.5$ | - | - |
| $\mathcal{B}(\times 10^{-6})$ | $38 \pm 2 \pm 2$ | $1.3 \pm 0.3 \pm 0.1$ | $192 \pm 8 \pm 29$ | $7.9 \pm 2.0 \pm 2.2$ | $230 \pm 8 \pm 30$ | $9.2 \pm 2.0 \pm 2.3$ |
| $\frac{\mathcal{B}(b \rightarrow d\gamma)}{\mathcal{B}(b \rightarrow s\gamma)}$ | $0.033 \pm 0.009 \pm 0.003$ | | | - | $0.040 \pm 0.009 \pm 0.010$ | |

TABLE III: Systematic errors on the measured partial and inclusive branching fractions \mathcal{B} . Systematic errors that do not cancel in the ratio of rates are marked with (*).

| Systematic Error Source | $M(X_s)$ | | $M(X_d)$ | |
|----------------------------------|----------|---------|----------|---------|
| | 0.5-1.0 | 1.0-2.0 | 0.5-1.0 | 1.0-2.0 |
| Track selection | 0.3% | 0.4% | 0.3% | 0.4% |
| Photon reconstruction | 1.8% | 1.8% | 1.8% | 1.8% |
| π^0/η reconstruction | 0.9% | 1.1% | 1.4% | 1.6% |
| Neural network | 1.1% | 4.9% | 1.1% | 4.9% |
| B counting | 0.6% | 0.6% | 0.6% | 0.6% |
| PID (*) | 2.0% | 2.0% | 2.0% | 2.0% |
| Fit bias (*) | 0.1% | 0.9% | 4.9% | 6.5% |
| PDF shapes (*) | 2.3% | 0.6% | 3.7% | 3.4% |
| Histogram binning (*) | 0.8% | 0.2% | 1.8% | 1.8% |
| Background (*) | 0.8% | 1.2% | 5.9% | 7.0% |
| Fragmentation (*) | - | 3.3% | - | 5.1% |
| Signal model | - | 5.8% | - | 6.0% |
| Error on partial \mathcal{B} | 4.0% | 9.0% | 9.3% | 14.2% |
| Missing ≥ 5 body | | 9.6% | | 18.2% |
| Other missing states | | 7.5% | | 15.3% |
| Spectrum Model | | 1.8% | | 1.6% |
| Error on inclusive \mathcal{B} | 4.0% | 15.2% | 9.3% | 27.7% |

hadronic final states with a mix of resonances; varying $b \rightarrow s\gamma$ fragmentation constraints within their statistical uncertainties; and setting the $b \rightarrow d\gamma$ fragmentation rates to those of their corresponding $b \rightarrow s\gamma$ states. The resulting missing fractions vary by up to 50(40)% relative to the nominal model in $B \rightarrow X_s\gamma(B \rightarrow X_d\gamma)$. We therefore independently vary final states with ≥ 5 stable hadrons, or with $\geq 2\pi^0$ or η mesons, by $\pm 50(40)\%$.

Results for the corrected \mathcal{B} values are shown in Table II. Adding the two mass regions, taking into account a partial cancellation of the missing fraction uncertainties in the ratio of $b \rightarrow d\gamma$ to $b \rightarrow s\gamma$, we find $\mathcal{B}(b \rightarrow d\gamma)/\mathcal{B}(b \rightarrow s\gamma) = 0.040 \pm 0.009(stat.) \pm 0.010(syst.)$ in the mass range $M(X) < 2.0 \text{ GeV}/c^2$.

We correct for the unmeasured region $M(X) > 2.0 \text{ GeV}/c^2$ using the spectral shape from Kagan-Neubert [18] with the kinetic parameters $(m_b, \mu_\pi^2) =$

$(4.65 \pm 0.05, -0.52 \pm 0.08)$ extracted from fits of $b \rightarrow s\gamma$ and $b \rightarrow c\ell\nu$ data [19], yielding corrections of 1.66 ± 0.03 ; the spectra for $b \rightarrow s\gamma$ and $b \rightarrow d\gamma$ are expected to be almost identical.

Conversion of the ratio of inclusive branching fractions to the ratio $|V_{td}/V_{ts}|$ is done according to [6], which requires the Wolfenstein parameters $\bar{\rho}$ and $\bar{\eta}$ as input. However, since the world average of these quantities relies on previous measurements of $|V_{td}/V_{ts}|$ we instead re-express $\bar{\rho}$ and $\bar{\eta}$ in terms of the world average of the independent CKM angle β [15]. This procedure yields a value of $|V_{td}/V_{ts}| = 0.199 \pm 0.022(stat.) \pm 0.024(syst.) \pm 0.002(th.)$, compatible and competitive with more model-dependent determinations from the measurement of the exclusive modes $B \rightarrow (\rho, \omega)\gamma$ and $B \rightarrow K^*\gamma$ [4, 5].

In summary, we have measured the inclusive $b \rightarrow s\gamma$ and $b \rightarrow d\gamma$ transition rates using a sum of seven final states in the hadronic mass range up to $2.0 \text{ GeV}/c^2$, making the first significant observation of the $b \rightarrow d\gamma$ transition in the region above $1.0 \text{ GeV}/c^2$. The value of $|V_{td}/V_{ts}|$ derived from these measurements has an experimental uncertainty approaching that from the measurement of exclusive decays $B \rightarrow (\rho, \omega)\gamma$ and $B \rightarrow K^*\gamma$, but a significantly smaller theoretical uncertainty.

I. ACKNOWLEDGMENTS

We are grateful for the excellent luminosity and machine conditions provided by our PEP-II colleagues, and for the substantial dedicated effort from the computing organizations that support BABAR. The collaborating institutions wish to thank SLAC for its support and kind hospitality. This work is supported by DOE and NSF (USA), NSERC (Canada), CEA and CNRS-IN2P3 (France), BMBF and DFG (Germany), INFN (Italy), FOM (The Netherlands), NFR (Norway), MES (Russia), MICINN (Spain), STFC (United Kingdom). Individuals have received support from the Marie Curie EIF (European Union), the A. P. Sloan Foundation (USA) and the Binational Science Foundation (USA-Israel).

[1] S. Bertolini, F. Borzumati, and A. Masiero, Nucl. Phys. B **294**, 321 (1987); H. Baer and M. Brhlik, Phys. Rev.

D **55**, 3201 (1997); J. Hewett and J. Wells, Phys. Rev. D **55**, 5549 (1997); M. Carena *et al.* Phys. Lett. B **499**,

- 141 (2001).
- [2] P. Ball, G. Jones and R. Zwicky, Phys. Rev. D **75**, 054004 (2007).
- [3] A. Abulencia *et al.* [CDF Collaboration], Phys. Rev. Lett. **97**, 242003 (2006).
- [4] D. Mohapatra *et al.* [Belle Collaboration], Phys. Rev. Lett. **96**, 221601 (2006).
- [5] B. Aubert *et al.* [BABAR Collaboration], Phys. Rev. Lett. **98**, 151802 (2007).
- [6] A. Ali, H. Asatrian and C. Greub, Phys. Lett. B **429**, 87 (1998).
- [7] B. Aubert *et al.* [BABAR Collaboration], Nucl. Instrum. Methods A **479**, 1 (2002).
- [8] B. Aubert *et al.* [BABAR Collaboration], Phys. Rev. Lett. **102**, 161803 (2009).
- [9] G. C. Fox and S. Wolfram, Nucl. Phys. B **149**, 413 (1979).
- [10] L-moments are defined as $L_i \equiv \sum_j p_j^* \cdot |\cos \theta_j^*|^i / \sum_j p_j^*$ and $\tilde{L}_i \equiv \sum_j p_j^* \cdot |\sin \theta_j^*|^i / \sum_j p_j^*$, where p_j^* and θ_j^* are the momentum and angle with respect to a given axis, respectively, for each particle j in the ROE.
- [11] B. Aubert *et al.*, [BABAR Collaboration], Phys. Rev. Lett. **89**, 201802 (2002).
- [12] M. J. Oreglia, Ph.D Thesis, SLAC-236, Appendix D (1980); J. E. Gaiser, Ph.D Thesis, SLAC-255, Appendix F (1982); T. Skwarnicki, Ph.D Thesis, DESY F31-86-02, Appendix E (1986).
- [13] The Cruijff function is a centered Gaussian with different left-right resolutions and non-Gaussian tails: $f(x) = \exp(-(x-m)^2 / (2\sigma_{L,R}^2 + \alpha_{L,R}(x-m)^2))$.
- [14] H. Albrecht *et al.* [ARGUS Collaboration], Phys. Lett. B **185**, 218 (1987).
- [15] Heavy Flavor Averaging Group, E. Barberio *et al.* arXiv:0704.3575 (hep-ex) (2007).
- [16] T. Sjöstrand, hep-ph/9508391; T. Sjöstrand, Comput. Phys. Commun. **82**, 74 (1994).
- [17] B. Aubert *et al.* [BABAR Collaboration], Phys. Rev. D **72**, 052005 (2005).
- [18] A. L. Kagan and M. Neubert, Phys. Rev. D **58**, 094012 (1998).
- [19] O. Buchmüller and H. Flächer, Phys. Rev. D **73**, 073008 (2006).